Pharmaceutical Research, Vol. 22, No. 2, February 2005 (© 2005)
DOI: 10.1007/s11095-004-1187-1

Research Paper

A Polymeric Nanoparticle Consisting of mPEG-PLA-Toco and PLMA-COONa as a Drug Carrier: Improvements in Cellular Uptake and Biodistribution

Yilwoong Yi,[1,2] Jae Hong Kim,[1] Hye-Won Kang,[1] Hun Seung Oh,[1] Sung Wan Kim,[3] and Min Hyo Seo[1,4]

Received July 9, 2004; accepted November 2, 2004

Purpose. To evaluate a new polymeric nanoparticulate drug delivery formulation that consists of two components: i) an amphiphilic diblock copolymer having tocopherol moiety at the end of the hydrophobic block in which the hydrophobic tocopherol moiety increases stability of hydrophobic core of the nanoparticle in aqueous medium; and ii) a biodegradable copolyester having carboxylate end group that is capable of forming ionic complex with positively charged compounds such as doxorubicin.
Methods. A doxourubicin-loaded polymeric nanoparticle (Dox-PNP) was prepared by solvent evaporation method. The entrapment efficiency, size distribution, and *in vitro* release profile at various pH conditions were characterized. *In vitro* cellular uptake was investigated by confocal microscopy, flow cytometry, and MTT assay using drug-sensitive and drug-resistant cell lines. Pharmacokinetics and biodistribution were evaluated in rats and tumor-bearing mice.
Results. Doxorubicin (Dox) was efficiently loaded into the PNP (higher than 95% of entrapment efficiency), and the diameter of Dox-PNP was in the range 20~25 nm with a narrow size distribution. *In Vitro* study showed that Dox-PNP exhibited higher cellular uptake into both human breast cancer cell (MCF-7) and human uterine cancer cell (MES-SA) than free doxorubicin solution (Free-Dox), especially into drug-resistant cells (MCF-7/ADR and MES-SA/Dx-5). In pharmacokinetics and tissue distribution study, the bioavailability of Dox-PNP calculated from the area under the blood concentration-time curve (AUC) was 69.8 times higher than that of Free-Dox in rats, and Dox-PNP exhibited 2 times higher bioavailability in tumor tissue of tumor-bearing mice.
Conclusions. Dox-PNP exhibited enhanced cellular uptake of the drug. In the cytotoxic activity study, this improved cellular uptake was proved to be more advantageous in drug-resistant cell. Dox-PNP exhibited much higher bioavailability in blood plasma and more drug accumulation in tumor tissue than conventional doxorubicin formulation. The results of this study suggest that the PNP system is an advantageous carrier for drug delivery.

KEY WORDS: biodistribution; cellular uptake; doxorubicin; multidrug resistant tumors; nonoparticles.

INTRODUCTION

Recently, great efforts have been made to develop nanoparticulate drug carriers such as nanoparticles, nanocapsules, micelles, liposomes, and conjugates (1,2,3). A major obstacle of nanoparticulate systems for drug delivery is extensive uptake of the particles by the reticuloendothelial systems (RES) (2,4,5). As a solution for avoiding the RES uptake, the surface of the nanoparticle was sterically stabilized by hydrophilic poly(ethylene glycol), and so-called "stealth particles" were developed (6).

Among various nanoparticulate drug carriers, polymeric micelles provide attractive characteristics in that they can avoid uptake of the drug by the RES *in vivo*, and hence, they can circulate in the blood for a long period of time. This advantage comes from the structure of a micelle: the hydrophilic portions of an amphiphilic block copolymer form the outer shell and are exposed to body fluid, and hence, the micelles can be protected from phagocytic cells and plasma proteins in the blood (7). Another important biological advantage of polymeric micelle is the EPR (enhanced permeability and retention) effect, or "passive targeting": polymeric micelles can slowly accumulate in malignant or inflamed tissues due to the elevated levels of vascular permeability factors in such cells. (8–11).

Critical micelle concentration (CMC) is the key param-

[1] Parenteral Delivery Research, Samyang R&D Center, Yuseong-Gu, Daejeon 305-717, South Korea.
[2] National Research Laboratory of Pharmaceutical Technology, College of Pharmacy, Chungnam National University, Yuseong-Gu, Daejeon 305-764, South Korea.
[3] Department of Pharmaceutics and Pharmaceutical Chemistry, Center for Controlled Chemical Delivery, University of Utah, Salt Lake City, Utah 84112-9452, USA.
[4] To Whom correspondence should be addressed. (e-mail: seo@samyang.com)

ABBREVIATIONS: Dox-PNP, doxorubicin-containing polymeric nanoparticle; Free-Dox, aqueous solution of doxorubicin hydrochloride; mPEG-PLA-Toco, methoxy poly(ethylene glycol)-*b*-poly(lactic acid) having a tocopherol moiety at the end of hydrophobic block; PLMA-COONa, sodium salt of poly (lactic acid-*co*-mandelic acid); PNP, polymeric nanoparticle.

eter for the formation and the physical stability of polymeric micelles. In aqueous media, amphiphlic polymers can exist in the form of micelles when the concentration is higher than CMC, and when diluted below this concentration, the micelles are collapsed and the drugs are liberated from the micelles. Although polymeric micelles would seem to be ideal carriers for poorly water-soluble drugs because of their distinct advantages, such as high solubility, long circulation of a drug in blood, permeation of an anticancer drug by the EPR effect, and simple sterilization, they have two major disadvantages in that physical instability upon dilution limits their application for pharmaceutical use, and water-soluble drugs cannot be incorporated in the micelles.

Doxorubicin, an anthracycline drug widely used to treat various types of cancer, is a fluorescent compound to be monitored easily by fluorescence detectors. In this paper, a polymeric nanoparticle containing doxorubicin was introduced. The physical characteristics, intracellular uptake behavior into both drug-sensitive and drug-resistant cell lines, and biodistribution of a doxorubicin-loaded polymeric nanoparticle (Dox-PNP) were investigated.

MATERIALS AND METHODS

Materials and Cell Lines

Dox (doxorubicin hydrochloride) was purchased from Sigma-Aldrichi Chemical Corp.(St. Louis, MO, USA). Other chemicals were of reagent grade and used as received.

Human breast carcinoma MCF-7 cells and their MDR variant MCF-7/ADR (NCI/ADR-RES) were obtained from ATCC (Manassas, VA, USA) and NCI (Frederick, MD, USA), respectively. MES-SA human uterine sarcoma cells, their MDR cells (MES-SA/Dx-5), and a human ovarian cancer cell line SKOV-3 were obtained from ATCC.

Synthesis of Amphiphilic Block Copolymer (mPEG-PLA-Toco)

The monomethoxy poly(ethylene glycol)-poly(lactic acid)-monomethoxy poly(ethylene glycol)-*b*-poly(lactic acid) (mPEG-PLA-OH) was synthesized by the ring-opening polymerization of DL-lactide in the presences of mPEG with a catalyst, stannous octoate, as described elsewhere (12,13). Next, the amphiphilic diblock copolymer shown in Fig. 1, mPEG-PLA-Toco, was synthesized by the reaction of mPEG-PLA-OH and DL-α-tocopherol succinate. The number average molecular weights of mPEG block and PLA block were 2000 and 1800, respectively.

Synthesis of Biodegradable Polyester (PLMA-COONa)

The biodegradable polyester, sodium salt of poly(lactic acid-*co*-mandelic acid) (PLMA-COONa), was synthesized by random copolymerization of DL-lactic acid and DL-mandelic acid. First, 7.5 g of DL-lactic acid (0.083 mol) and 2.5 g of DL-mandelic acid (0.016 mol) were added to a reactor equipped with a mechanical stirrer and a distillation set. Moisture was evaporated at 80°C for 1 h under reduced pressure (25 mmHg) with an aspirator. The reaction was carried out at an elevated temperature of 180°C for 5 h under vacuum (10 mmHg). The resulting product was added to distilled water, and the precipitated polymer was further washed with distilled water. The polymer product was then added to 0.1 L of distilled water, and the pH was adjusted to 6~8 by adding sodium hydrogen carbonate portionwise thereto to dissolve the polymer. The water-insoluble polymer was separated and removed by centrifugation or filtration. A 1 N hydrochloric acid solution was added dropwise thereto, and the polymer was precipitated again in the aqueous solution. The precipitated polymer was washed twice with distilled water, isolated, and dried under reduced pressure to obtain the polymer having carboxyl end group (6.7 g of PLMA-COOH, yield = 67%). The number average molecular weight of the polymer determined with NMR was 1100.

Next, 5 g of PLMA-COOH polymer was dissolved in acetone in a reactor equipped with a mechanical stirrer and a distillation set. The solution was stirred slowly at room temperature, and sodium hydrogen carbonate solution (1 N) was slowly added thereto to reach pH 7. Anhydrous magnesium sulfate was added thereto to remove water. The mixture was filtered, acetone was evaporated with a rotary evaporator, and white solid product was obtained. The solid product was dissolved again in anhydrous acetone, the solution was filtered to remove the insoluble particles, and acetone was evaporated to give the final product, PLMA-COONa, in white solid (yield: 95%).

Preparation of Doxorubicin-Loaded Polymeric Nanoparticle (Dox-PNP)

The doxorubicin-containing polymeric nanoparticles, Dox-PNP, were prepared as follows: Ten milligrams (0.017 mmol) of doxorubicin hydrochloride was dissolved in 5 ml of ethanol-water (9:1 v/v) in a round-bottomed flask. One hundred ninety milligrams (0.17 mmol) of the biodegradable polyester (PLMA-COONa) was added thereto and completely dissolved with a rotary evaporator at an elevated temperature of 50°C for 30 min to give a clear solution. Eight hundred ninety milligrams (0.21mmol) of the amphiphilic block copolymer (mPEG-PLA-Toco) was added and dissolved in the solution. The solvent was evaporated at an elevated temperature (50°C) under vacuum with a rotary evaporator. Three milliliters of an aqueous solution of lactose (20% by weight) was added, and the flask was rotated at 100 rpm to form the Dox-PNP colloidal solution in aqueous medium. The solution was filtered using 0.22-μm polyvinylidene

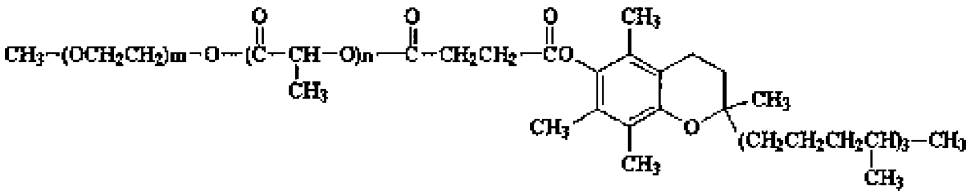

Fig. 1. Structural formula of mPEG-PLA-Toco.

fluoride (PVDF) membrane filter. The filtered solution was freeze-dried and stored in a refrigerator until use. Particle size of Dox-PNP was measured by dynamic light scattering method (DLS; ZetaPlus, Brookhaven Instruments Ltd., Holtsville NY, USA). The doxorubicin content was determined by high performance liquid chromatography (HPLC) (Hewlett Packard series 1100) using daunorubicin as the internal standard.

In Vitro Release

The drug release experiment was carried out *in vitro* at different pH conditions (phosphate buffer for pH 7.4 and acetate buffer for pH 5.0 and 3.0). Dox-PNP containing 3.0 mg of Dox was suspended in 2 ml buffer solution. The solution was poured into a dialysis bag (MWCO 3500). The dialysis bag was then placed in a bottle containing 150 ml of buffer solution. The bottle was placed in the shaking water bath and stirred at 37°C and 50 rpm. At the given time intervals, drug release from nanoparticles was measured by UV-Vis spectrophotometer (Beckman DU 650) at 485 nm.

Confocal Microscopy

To visualize the intracellular uptake of a drug, Dox-PNP and Free-Dox were tested for the human breast cancer cell lines MCF-7 (doxorubicin-sensitive cell line) and MCF-7/ADR (doxorubicin-resistant cell line). The cells were imaged on a Zeiss (Thornwood, NY, USA) LSM 510 confocal imaging system with an inverted fluorescence microscope and an image analyzer. Briefly, cells (3×10^5) in 3 ml of RPMI 1640 medium (Invitrogen Corp.) supplemented with 10% fetal bovine serum and 1% penicillin streptomycin were incubated overnight on a glass coverslip at 37°C. After incubation, cells were treated with the drug compositions at a dose of 1.0 μg/ml, and the coverslip was mounted on the microscope. At the given time intervals, the fluorescence was observed at an excitation wavelength of 484 nm.

Flow Cytometry

To evaluate the intracellular uptake of doxorubicin, flow cytometry study was performed with the FACStarPlus (Becton Dickinson) according to the method of Walker *et al.* (14). Briefly, cells (1.0×10^6) were incubated in culture medium for 24 h and were treated with the drug compositions at a dose of 1.0 μg/ml. Cells in 12 × 75 Falcon tubes were placed on the FACStarPlus, and the fluorescence was observed at wavelengths of 488 nm (excitation) and 519 nm (emission). Data were analyzed by CellQuest software.

In Vitro Cytotoxicity

For *in vitro* cytotoxic activity study, both drug-sensitive and drug-resistant cell lines were used: human breast cancer cell line MCF-7 and human uterine cancer cell line MES-SA as drug-sensitive cells and MCF-7/ADR and MES-SA/Dx-5 as drug-resistant cells. The cytotoxic activity was evaluated at five 10-fold dilutions ranging from 0.01 to 100 μg/ml. Following continuous exposure for 1, 2, and 3 days, cells were treated with MTT (methylthiazoletetrazolium), and the MTT-formazan produced from reduction of MTT-tetrazolium by the enzymes in living cells was detected by a fluorescence reader. The results were expressed as IC_{50} (50% inhibitory concentration) values of each cell line. The MTT assay was carried out as follows: Cells were harvested from exponential phase culture growing in RPMI 1640 medium (MCF7 and MCF7/ADR) or McCoy's 5A medium (MES-SA and MES-SA/Dx-5) supplemented with 10% fetal bovine serum and 1% penicillin streptomycin, counted and plated in 96-well flat-bottomed microtiter plates (5×10^4 cells/ml for each cell line). After a 24-h recovery to allow cells to resume exponential growth, culture medium (24 control wells per plate) or culture medium containing drug was added to the wells. Each drug concentration was plated in triplicate. Following 1, 2, and 3 days of continuous drug exposure, cells were treated with 25 μl of a MTT solution in sterile water (2 mg/ml). Fluorescence was measured using an automatic microplate reader (SpectraMax 190, Molecular Devices) at the wavelength of 549 nm, and the amount of viable cells was calculated from the optical density.

Pharmacokinetics and Tissue Distribution

Pharmacokinetics and tissue distribution of a drug were evaluated for Dox-PNP and Free-Dox in rats and tumor-bearing mice. Animal studies were consistent with the Principles of Laboratory Animal Care (NIH Publication No. 85-23, revised 1985).

Rats

The Sprague-Dawley rats (200~250 g) were injected intravenously through the tail vein at a dose of 5 mg/kg. Four rats were sacrificed at 0.5, 4, 12, and 24 h after drug administration. Samples of plasma, liver, kidneys, spleen, lungs, heart, and brain were collected, and the amount of doxorubicin was analyzed by the HPLC assay. The area under the concentration-time curve (AUC) was calculated using the linear trapezoidal rule.

Mice

Female athymic BALB/c (nu/nu) mice (20~25 g) were injected subcutaneously in the right flank with 0.1 ml of ell suspension containing 7×10^6 SKOV-3 human ovarian cancer cells. After the cancers reached a certain size, they were xenografted three times. The xenograft fragments (3~4 mm) were implanted subcutaneously into the mice in the right flank using 12-gauge trocar needles. Tumor sizes were measured every day, and the tumor volumes were calculated by the formula $(W^2 \times L)/2$, where W is a short axis and L is a long axis. When the tumor volumes reached 100~300 mm^3, the mice were injected intravenously through the tail vein at a dose of 10 mg/kg. Four mice were sacrificed at 0.5, 4, 24, 48, and 96 h after drug administration. Samples of plasma, liver, kidneys, spleen, lungs, heart, and tumor were collected, and the amount of doxorubicin was analyzed by the HPLC assay. The area under the concentration-time curve (AUC) was calculated using the linear trapezoidal rule.

RESULTS AND DISCUSSION

Characteristics of Dox-PNP

Doxorubicin was effectively incorporporated into the PNP (0.92% of loading, w/w) with an entrapment efficiency of 95.7%. PNP with very narrow size distribution ($d_w/d_n = 1.07$)

Table I. Characteristics of Dox-PNP

Initial loading							
Dox	PLMA-COONa	mPEG-PLA-Toco	% Loading (w/w)	Entrapment efficiency[a]	Weight-average diameter (d_w)	Number-average diameter (d_n)	d_w/d_n
10 mg	190 mg	890 mg	0.92%	95.7%	23.2 nm	21.7 nm	1.07

[a] Weight % of drug incorporated in Dox-PNP with respect to the initial drug used.

was formed as summarized in Table I. The weight-average and number-average diameters were 23.2 nm and 21.7 nm, respectively. Figure 2 shows the histograms of size distribution of Dox-PNP measured by dynamic light scattering (DLS).

As shown in the NMR spectra of Figs. 3(A) and 3(B), only mPEG peaks were dectected from Dox-PNP and PNP with no drug in D_2O. This indicates that only PEG on the surface of the nanoparticle can move freely in aqueous medium and the other components, hydrophobic block in mPEG-PLA-Toco, PLMA polymer, and the ionic complex of PLMA-Dox shown in Fig. 4, constitute the inner core of the PNP. This feature of Dox-PNP may provide two important advantages as a drug carrier: passive drug targeting by EPR effect can be achieved due to the small size of PNP; and the RES uptake can be avoided due to the sterically stabilized surface by the hydrophilic polymer surrounding the PNP (2).

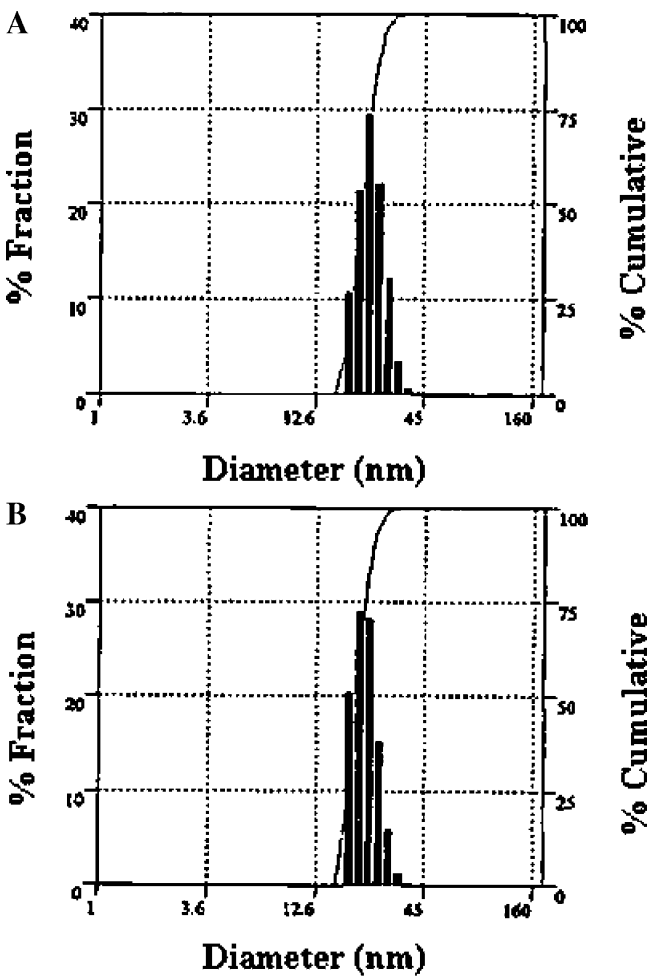

Fig. 2. Size distribution of Dox-PNP in aqueous medium measured by dynamic light scattering (DLS): (A) weight-average distribution and (B) number-average distribution.

In Vitro Release

Large molecules, such as nanoparticles, can be taken up by cells via endocytotic process (3,15,16). The fraction of administered nanoparticles taken up by endocytosis fuses with lysosomes, and the drug should escape the endolysomes into cytoplasm. Because the endolysosomal condition is more acidic (pH 4~5) than physiolosical condition (pH 7.4 in cytosol) (17,18), *in vitro* release of drug from Dox-PNP was compared at different pH conditions. As shown in Fig. 5, Dox was released pH-dependently: more stable in physiologic pH than in endolysosomal pH. This release profile indicates that Dox-PNP is stable at physiologic pH but the carboxylate anion ($PLMA\text{-}COO^-$) in the ionic complex ($PLMA\text{-}COO\text{-}H_3N\text{-}Dox$) is liberated as free acid form (PLMA-COOH) at low pH, and doxorubicin diffuses out to cytosol.

Confocal Microscopy

To achieve a desired therapeutic effect of a drug, an appropriate amount of the administered drug should enter the target cells in a body. In order to increase a cellular internalization of a drug, an appropriate concentration of the drug in the target tissue should be maintained for a desired time period, and further, the drug should enter the target cells in the tissue.

Using the intrinsic fluorescence of doxorubicin, the cellular uptake behavior of Dox-PNP in both drug-sensitive and drug-resistant cells was visualized and compared to Free-Dox by confocal laser scanning microscopy (19). Cellular uptake

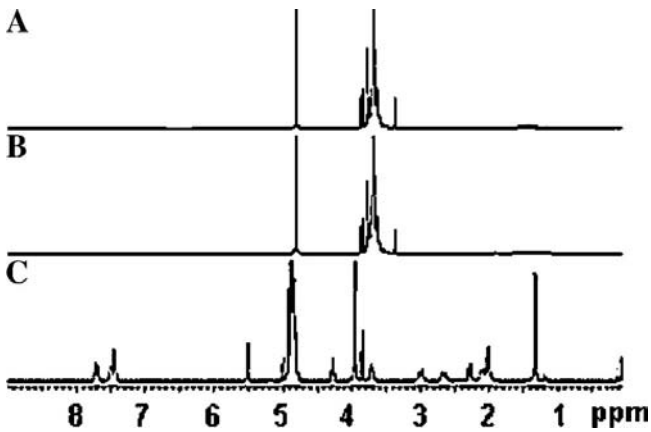

Fig. 3. ^{1}H-NMR spectra of (A) Dox-PNP, (B) PNP with no drug, (C) Free-Dox in D_2O.

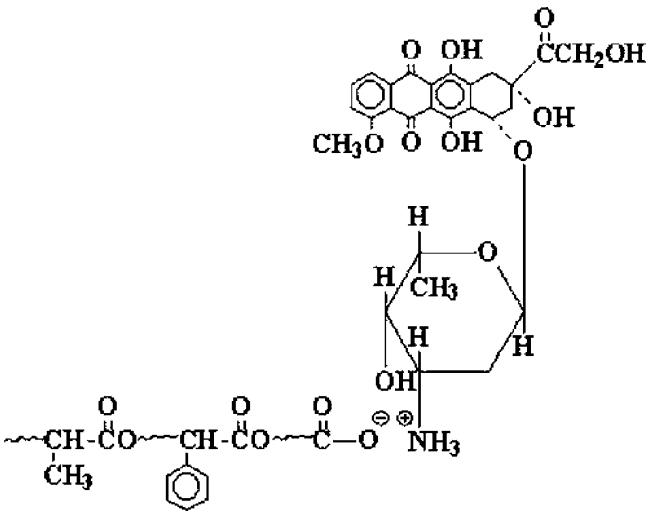

Fig. 4. Schematic structure for the ionic complex, PLMA-Dox.

of the drug in Dox-PNP was faster than that of Free-Dox into drug-sensitive cell line, MCF-7, as shown in Figs. 6(A) and 6(B). After 4 h of exposure, most of the cells treated with Dox-PNP exhibited fluorescence intensity corresponding to doxorubicin. The intensity became stronger after 8 h of exposure, and most of the cells died at 24 h after treatment. On the contrary, fluorescence intensity of the cells treated with Free-Dox was much weaker than Dox-PNP until 24 h after treatment. Further, considerable drug was taken up by the drug-resistant cells (MCF-7/ADR) when treated with Dox-PNP, but only a slight intensity was detected from Free-Dox, as shown in Figs. 6(C) and 6(D). This result implies that Dox-PNP delivers a drug into cells in different ways other than simple diffusion of Free-Dox.

Faster uptake and more amount of drug accumulation into the drug-resistant cells from Dox-PNP suggests an important biological implication in cancer chemotherapy. Cellular drug resistance is considered as one of the major reasons for failure of anticancer chemotherapy. Among various mechanisms of resistance to anthracyclines in tumor cells, the classic multidrug resistance (MDR) due to the presence of

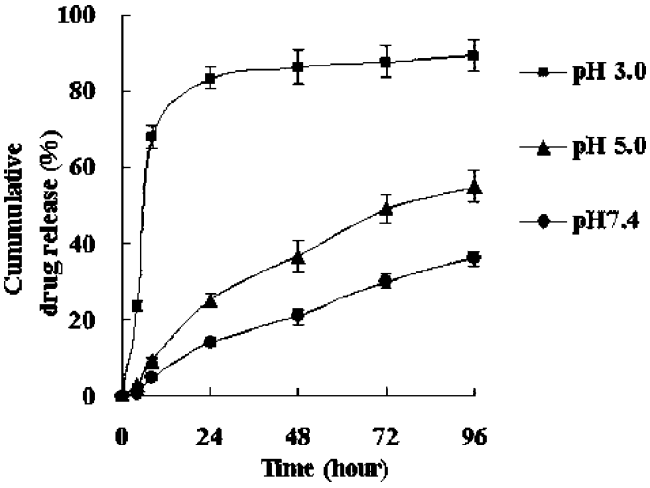

Fig. 5. pH-dependent release of Dox from Dox-PNP: The pHs 7.4 and 5.0 correspond to physiological and endolysomal conditions, respectively. Each point represents the mean ± SD of three experiments.

P-glycoprotein (P-gp) in plasma membrane is thought to be the primary factor (20), and P-gp is highly expressed in the MCF-7/ADR cells (21,22). Numerous researches have been made on the MDR-associated proteins, and the resistance that is not caused by the "classic" P-gp is designated as "atypical" MDR (22–24). From the result of cellular uptake into MDR cell line, it is suggested that Dox-PNP has a potential for treating multidrug-resistant tumors.

Flow Cytometry

The cellular uptake behavior of Dox-PNP in both drug-sensitive and drug-resistant cells was evaluated from the fluorescence histograms obtained from flow cytometry. To quantify the degree of cellular uptake, %Cells and ΔIntensity were calculated from the fluorescence intensity data: The intensity corresponding to approximately 1% of cell counts in the upper intensity at initial time (0 h) in the fluorescence histograms was marked (marker bar), and %Cells was determined as the fraction (%) of cell counts coming into the area of the marker bar at given time. This value corresponds to the number of cells by which drug was taken up. ΔIntensity was determined by the increased fluorescence intensity at given time from initial time (0 h), and the value correlates with the total amount of drug taken up by the cells.

As shown in Table II, Dox-PNP exhibited higher cellular uptake than Free-Dox when treated with drug-sensitive cells (MCF-7): at 8 h incubation, %Cells were 63.0 for Dox-PNP and 42.9 for Free-Dox, and ΔIntensity for Dox-PNP was 1.4 times higher than Free-Dox. When treated with drug-resistant cells (MCF-7/ADR) the difference in cellular uptake was much greater than with drug-sensitive cells: at 8 h incubation, %Cells were 21.3 for Dox-PNP and 8.6 for Free-Dox, and ΔIntensity for Dox-PNP was 2.6 times higher than Free-Dox. The fluorescence intensity in MCF-7/ADR cells from the physical mixture of PNP and Free-Dox was almost identical to that from Free-Dox, and it seems that empty PNP or its degradation products do not affect the transport of drug into cells.

More promising results were obtained from human uterine cancer cells (MES-SA and MES-SA/Dx-5). As shown in Table III, Dox-PNP exhibited higher cellular uptake than Free-Dox when treated with drug-sensitive cells (MES-SA): at 8 h after treatment, %Cells were 92.3 for Dox-PNP and 35.1 for Free-Dox, and ΔIntensity for Dox-PNP was 2.6 times higher than Free-Dox. Further, for the drug-resistant cells (MES-SA/Dx-5), the difference in cellular uptake became dramatically increased: at 8 h after incubation, %Cells were 29.3 for Dox-PNP and 5.3 for Free-Dox, and ΔIntensity for Dox-PNP was 5.0 times higher than Free-Dox. The values for Dox-PNP in drug-resistant cells were comparable to those for Free-Dox in drug-sensitive cells. In both drug-resistant cells (MCF-7/ADR and MES-SA/Dx-5), Free-Dox was not practically taken up by the cells, whereas Dox-PNP delivered considerable amount of drug into the drug-resistant cells.

The results of flow cytometry study on cellular uptake agree to those from the confocal microscopy, and the PNP formulation might be a candidate of a drug carrier for treating multidrug-resistant tumors.

In Vitro Cytotoxicity

In vitro cytotoxic activity was done by MTT assay, and the results are summarized in Table IV. The vehicle for Dox-

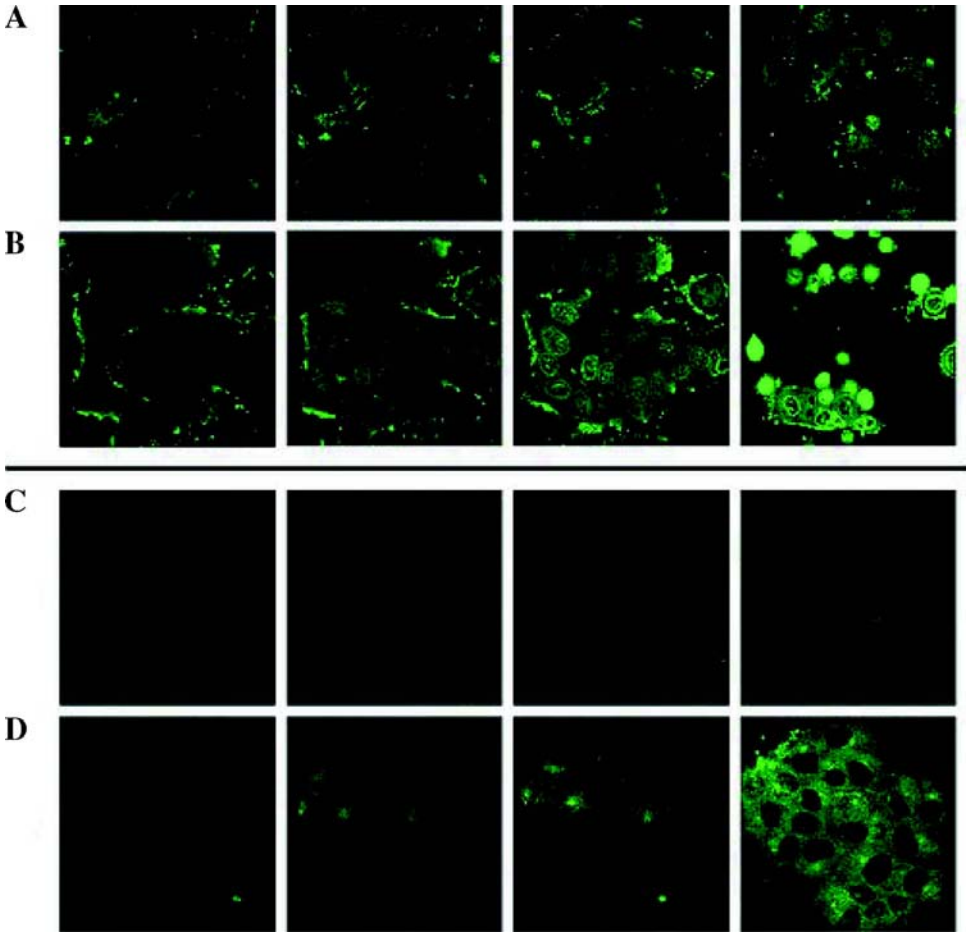

Fig. 6. Confocal laser scanning microscopy (CLSM) images of MCF-7 and MCF-7/ADR cells after exposure of 2, 4, 8, and 24 h (from left to right). (A) Free-Dox in MCF-7, (B) Dox-PNP in MCF-7, (C) Free-Dox in MCF-7/ADR, and (D) Dox-PNP in MCF-7/ADR.

PNP showed no cytotoxicity at all the concentrations tested (0.01 to 100 μg/ml). The IC_{50} values for the drug-sensitive cells was similar in both compositions of Free-Dox and Dox-PNP, but the Dox-PNP showed 38.1 (MCF-7/ADR) and 5.4 (MES-SA/Dx-5) times higher activity at 3 days after treatment than Free-Dox when treated onto the drug-resistant cells. These results support the results of flow cytometry and confocal microscopy.

As shown in Fig. 7, cell viability of Dox-PNP was 2.7 times lower than that of Free-Dox when treated on MCF-7/ADR. When treated on MES-SA/Dx-5, viability of Dox-PNP was 6.8 times lower than that of Free-Dox (data not shown). This difference in the cytotoxic activity between drug-sensitive and drug-resistant cells is due to the characteristics of the drug-resistant cells in which the MDR-associated membrane transporters are overexpressed, and they continuously

Table II. Cellular Uptake of Doxorubicin into Human Breast Cancer Cells (Concentration: 1.0 μg/ml)

Exposure time	% Cells[a]			ΔIntensity[b] (× 10)		
	Cell lines	Free-Dox	Dox-PNP	Cell lines	Free-Dox	Dox-PNP
0 h	MCF-7	1.0	1.0	MCF-7	0.0	0.0
1 h		1.7	9.1		8.2	47.0
4 h		17.3	39.4		73.7	120.4
8 h		42.9	63.0		128.4	177.6
0 h	MCF-7/ADR	1.0	1.0	MCF-7/ADR	0.0	0.0
1 h		1.3	7.0		1.6	17.7
4 h		4.2	14.6		8.5	27.3
8 h		8.6	21.3		16.0	41.9

[a] Fraction (%) of cell counts by which drug was taken up.
[b] Increase of fluorescence intensity at given time from initial time (0 h).

Table III. Cellular Uptake of Doxorubicin into Human Uterine Cancer Cells (Concentration: 1.0 μg/ml)

Exposure time	% Cells[a]			ΔIntensity[b] (× 10)		
	Cell lines	Free-Dox	Dox-PNP	Cell lines	Free-Dox	Dox-PNP
0 h	MES-SA	1.0	1.0	MES-SA	0.0	0.0
1 h		4.0	16.3		7.6	25.6
4 h		11.3	68.9		20.6	68.8
8 h		35.1	92.3		40.9	108.3
0 h	MES-SA/Dx-5	1.0	1.0	MES-SA/Dx-5	0.0	0.0
1 h		1.8	10.4		2.6	23.4
4 h		3.2	22.7		7.1	37.6
8 h		5.3	29.3		9.2	46.2

[a] Fraction (%) of cell counts by which drug was taken up.
[b] Increase of fluorescence intensity at given time from initial time (0 h).

extrude the drug from the cells. Because free drug cannot be concentrated within the drug-resistant cells, the higher cytotoxic activity of Dox-PNP over Free-Dox implies that the cellular uptake of doxorubicin from Dox-PNP includes different transport process other than simple diffusion, such as endocytosis of the nanoparticles.

Endocytotic uptake of nanoparticles can be categorized nonspecific fluid-phase endocytosis, adsorptive endocytosis, and specific receptor-mediated endocytosis (RME) (15,25). Maysinger *et al.* explained that cellular internalization of poly(caprolactone)-*b*-poly(ethylene oxide) (PCL-PEO) block copolymer micelles was endocytotic by showing the time, temperature, pH, and energy-dependent properties of the process (26,27). On the other hand, in a series of articles, Couvreur *et al.* elucidated the cellular uptake mechanism from doxorubicin-loaded polyalkylcyanoacrylate (PACA) nanoparticles: the nanoparticles are adsorbed on the cell membrane, and then the ion pairs of doxorubicin-poly(cyanoacrylic acid) complex penetrate the cell membrane (28–35).

Although the carboxylate anion in Dox-PNP (PLMA-COO^-) forms an ionic complex (PLMA-COO-H_3N-Dox) with doxorubicin in aqueous medium like the ion pairs of doxorubicin-poly(cyanoacrylic acid) in PACA nanoparticulate system, the surface of Dox-PNP is somewhat different from that of PACA nanoparticle in that Dox-PNP forms a hydrophilic outer shell consisting of hydrophilic PEG and carboxylate anion (PLMA-COO^-) in aqueous medium like PCL-PEO block copolymer micelles. In consideration of this point, it is suggested that endocytosis of Dox-PNP be incorporated in the cellular uptake process.

Pharmacokinetics and Biodistribution

The pharmacokinetics and biodistribution study was performed with Sprague-Dawley rats (200~250 g) and nude(nu/nu) athymic mice (20~25 g) bearing tumor tissues, and the results are shown in Tables V and Fig. 8.

In rats, the bioavailability calculated from the area under the blood concentration-time curve (AUC) for Dox-PNP was 69.8 times higher than that for Free-Dox. In addition, the AUC in heart was less than half for Dox-PNP compared to Free-Dox. Because the major side effect of doxorubicin is considered as heart failure (26), this result implies another advantage of Doxo-PNP over Free-Dox. AUCs of Dox-PNP in liver and spleen, the major RES uptake organs, were higher than those of Free-Dox as seen in most colloidal drug carriers (6,16,36).

In tumor-bearing mice, the results of biodistribution were similar to the results in rats: AUCs of Dox-PNP compared to those of Free-Dox were higher in blood plasma, liver, and spleen; and lower in heart and kidney. As shown in Fig. 8, Dox-PNP exhibited prolonged blood circulation time compared to the Free-Dox: the AUC for Dox-PNP was 11.4 times higher than that for Free-Dox. Further, the AUC for Dox-PNP in tumor tissue was two times higher than that for Free-Dox.

CONCLUSIONS

A polymeric nanoparticle system consisting of mPEG-PLA-Toco and PLMA-COONa was proved to be a potential drug carrier. The particle size was suitable for EPR effect in

Table IV. *In Vitro* Cytotoxicity of Dox-PNP and Free Doxorubicin, IC_{50}[a]

Exposure time	Drug-sensitive cells			Drug-resistant cells		
	Cell lines	Free-Dox	Dox-PNP	Cell lines	Free-Dox	Dox-PNP
24 h	MCF-7	21.7	1.02	MCF-7/ADR	>100	19.6
48 h		0.35	0.10		43.0	1.1
72 h		0.14	0.04		26.7	0.7
24 h	MES-SA	0.30	0.14	MES-SA/Dx-5	54.0	0.95
48 h		0.087	0.068		0.92	0.28
72 h		0.031	0.018		0.75	0.14

[a] IC_{50} inhibitory concentration of doxorubicin producing 50% of cell growth.

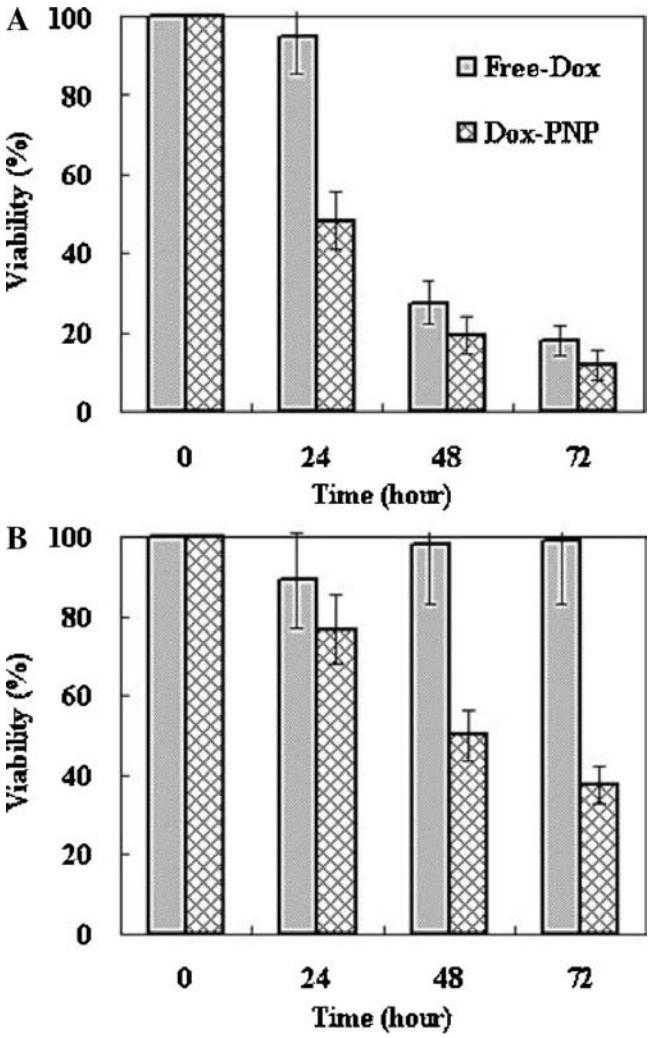

Fig. 7. Cell viability after treatment of Free-Dox and Dox-PNP at a drug concentration of 1.0 μg/ml on (A) MCF-7 and on (B) MCF-7/ADR. Each bar represents the mean ± SD of three experiments.

tumor tissues, and drug was efficiently incorporated into the PNP. Confocal images and flow cytometry showed enhanced cellular uptake of the drug. From the result of cytotoxic activity study, this improved cellular uptake proved to be more

Table V. Tissue Distribution of Doxorubicin in Rats at a Dose of 5 mg/kg

	Free-Dox		Dox-PNP		
Tissue	AUC_{0-24}[a]	T/P ratio[b]	AUC_{0-24}[a]	T/P ratio[b]	Ratio[c]
Plasma	1.5	1.0	104.7	1.0	69.8
Heart	17.9	11.9	6.4	0.06	0.4
Liver	91.4	60.9	881.4	8.4	9.6
Spleen	563.9	375.9	10,731.5	102.5	19.0
Kidney	934.3	622.9	572.0	5.5	0.6
Lungs	84.7	56.5	126.5	1.2	1.5
Brain	1.9	1.3	5.4	0.05	2.8

[a] AUC_{0-24} (μg · h/ml or μg · h/g), area under the drug concentration-time curve from 0 to 24 h.
[b] Tissue-to-plasma ratio based on AUCs.
[c] Ratio of AUCs (Dox-PNP to Free-Dox).

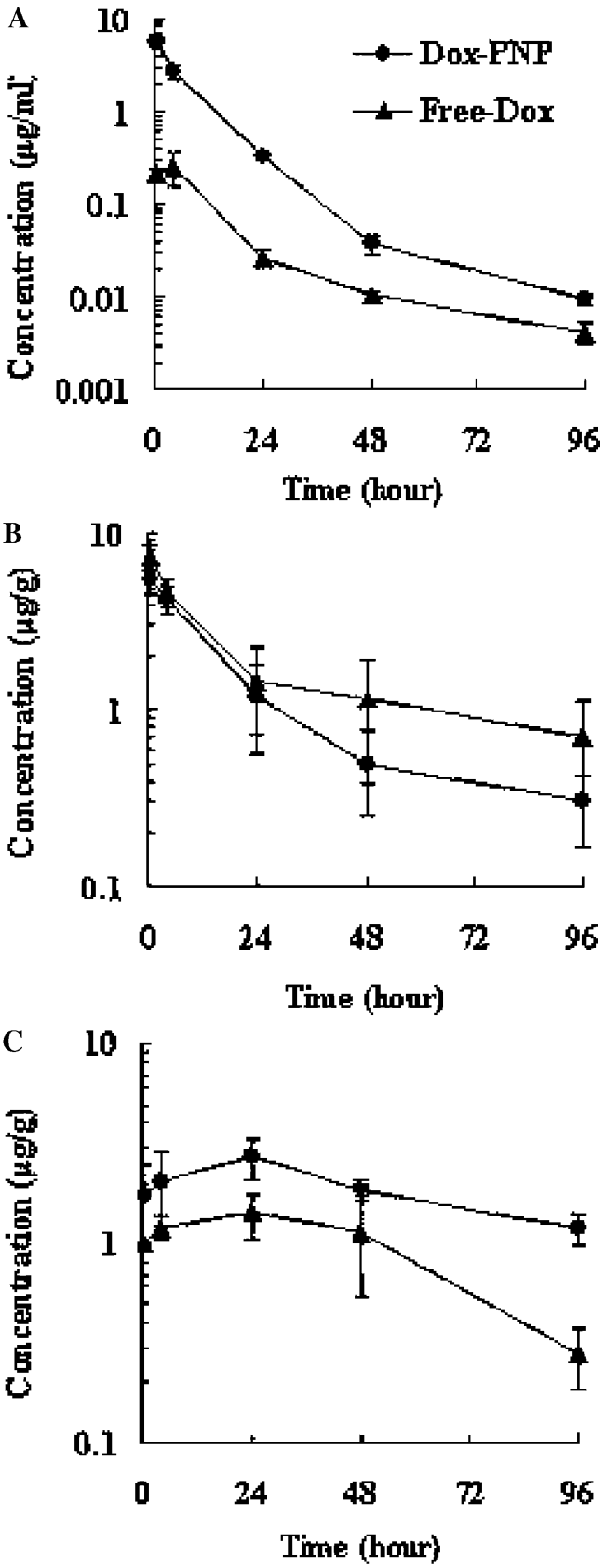

Fig. 8. Tissue distribution of doxorubicin in mice at a dose of 10 mg/kg: (A) blood, (B) heart, and (C) tumor. Each point represents the mean ± SD of four mice.

advantageous in drug-resistant cells. In pharmacokinetics and tissue distribution study, Dox-PNP exhibited much higher bioavailability in blood plasma and more drug accumulation than conventional doxorubicin formulation. The results of this study shows that Dox-PNP appears to be a promising formulation, having improved cellular uptake and biodistribution of a drug, and the complete elucidation of the mechanism of PNP-induced cellular uptake remains for further study.

REFERENCES

1. V. P. Torchilin and V. S. Trubetskoy. Which polymers can make nanoparticulate drug carriers long-circulating? *Adv. Drug Deliv. Rev.* **16**:141–155 (1995).
2. M.-C. Jones and J.-C. Leroux. Polymeric micelles—a new generation of colloidal drug carriers. *Eur. J. Pharm. Biopharm.* **48**: 101–111 (1999).
3. J. Panyam and V. Labhasetwar. Biodegradable nanoparticles for drug and gene delivery to cells and tissue. *Adv. Drug Deliv. Rev.* **55**:329–347 (2003).
4. K. Kataoka, T. Matsumoto, M. Yokoyama, T. Okano, Y. Sakurai, S. Fukushima, K. Okamoto, and G. S. Kwon. Doxorubicin-loaded poly(ethylene glycol)-poly(β-benzyl-L-aspartate) copolymer micelles: their pharmaceutical characteristics and biological significance. *J. Control. Rel.* **64**:143–153 (2000).
5. V. Alakhov, E. Klinski, S. Li, G. Pietrzynski, A. Venne, E. Batrakova, T. Bronitch, and A. Kabanov. Block-copolymer-based formulation of doxorubicin. From cell screen to clinical trials. *Colloids Surf. B Biointerfaces* **16**:113–134 (1999).
6. G. M. Barratt. Therapeutic applications of colloidal drug carriers. *Pharm. Sci. Technol. Today* **3**:163–171 (2000).
7. V. Torchilin. Structure and design of polymeric surfactant-based drug delivery systems. *J. Control. Rel.* **73**:137–172 (2001).
8. H. Maeda. The tumor blood vessel as an ideal target for macromolecular anticancer agents. *J. Control. Rel.* **19**:315–324 (1992).
9. T. N. Palmer, V. J. Caride, M. A. Caldecourt, J. Twickler, and V. Abdullah. The mechanism of liposome accumulation in infarction. *Biochim. Biophys. Acta* **797**:363–368 (1984).
10. A. A. Gabizon. Liposome circulation time and tumor targeting: implications for cancer chemotherapy. *Adv. Drug Deliv. Rev.* **16**: 285–294 (1995).
11. H. Maeda, J. Wu, T. Sawa, Y. Matsumura, and K. Hori. Tumor vascular permeability and the EPR effect in macromolecular therapeutics: a review. *J. Control. Rel.* **65**:271–284 (2000).
12. K. J. Zhu, L. Xiangzhou, and Y. Shinlin. Preparation, characterization, and properties of polylactide (PLA)-poly(ethylene glycol) (PEG) copolymers: A potential drug carrier. *J. Appl. Polym. Sci.* **39**:1–9 (1990).
13. B. Jeong, Y. H. Bae, D. S. Lee, and S. W. Kim. Biodegradable block copolymers as injectable drug-delivery systems. *Nature* **388**: 860–862 (1997).
14. P. R. Walker, J. Kwast-Welfeld, H. Gourdeau, J. Leblanc, W. Neugebaur, and M. Sikorska. Relationship between apoptosis and the cell cycle in lymphocytes: roles of protein kinase C, tyrosine phosphorylation, and AP1. *Exp. Cell Res.* **207**:142–151 (1993).
15. Y. Kakizawa and K. Kataoka. Block copolymer micelles for delivery of gene and related compounds. *Adv. Drug Deliv. Rev.* **54**:203–222 (2002).
16. I. Brigger, C. Dubernet, and P. Couvreur. Nanoparticles in cancer therapy and diagnosis. *Adv. Drug Deliv. Rev.* **54**:631–651 (2002).
17. Y. Bae, S. Fukushima, A. Harada, and K. Kataoka. Design of environment-sensitive supramolecular assemblies for intracellular drug delivery: polymeric micelles that are responsive to intracellular pH change. *Angew. Chem. Int. Ed. Engl.* **42**:4640–4643 (2003).
18. J. Panyam, W.-Z. Zhou, S. Prabha, S. K. Sahoo, and V. Labhasetwar. Rapid endo-lysosomal escape of poly(DL-lactide-coglycolide) nanoparticles: implications for drug and gene delivery. *FASEB J.* **16**:1217–1226 (2002).
19. V. Omelyanenko, P. Kopečková, C. Gentra, and J. Kopeček. Targetable HPMA copolymer-adriamycin conjugate. Recognition, internalization, and subcellular fate. *J. Control. Rel.* **53**:25–37 (1998).
20. D. Nielsen, C. Maare, and T. Skovsgaard. Cellular resistance to anthracyclines. *Gen. Pharmacol.* **27**:251–255 (1996).
21. L. M. Leoni, E. Hamel, D. Genini, H. Shih, C. J. Carrera, H. B. Cottam, and D. A. Carson. Indanocine, a microtubule-binding indanone and a selective inducer of apoptosis in multidrug-resistant cancer cells. *J. Natl. Cancer Inst.* **92**:217–224 (2000).
22. D. A. Scudiero, A. Monks, and E. A. Sausville. Cell line designation change: Multidrug-resistant cell line in the NCI anticancer screen. *J. Natl. Cancer Inst.* **90**:862 (1998).
23. H. Lage and M. Dietel. Effect of the breast-cancer resistance protein on atypical multidrug resistance. *Lancet Oncol.* **1**:169–175 (2000).
24. D. D. Ross, W. Yang, L. V. Abruzzo, W. S. Dalton, E. Schneider, H. Lage, M. Dietel, L. Greenberger, S. P. C. Cole, and L. A. Doyle. Atypical multidrug resistance: breast cancer resistance protein messenger RNA expression in mitoxantrone-selected cell lines. *J. Natl. Cancer Inst.* **91**:429–433 (1999).
25. A. J. Vander, J. H. Sherman, and D. S. Luciano. Movements of molecules across cell membranes. In A. J. Vander, J. H. Sherman, and D.S. Luciano (eds.), *Human Physiology,* 6th Ed., McGraw-Hill, New York, 1994, pp. 115–145.
26. C. Allen, Y. Yu, A. Eisenberg, and D. Maysinger. Cellular internalization of PCL20-b-PEO44 block copolymer micelles. *Biochim. Biophys. Acta* **1421**:32–38 (1999).
27. R. Savic, L. Luo, A. Eisenberg, and D. Maysinger. Micellar nanocontainers distribute to defined cytoplasmic organelles. *Science* **300**:615–618 (2003).
28. C. Vauthier, C. Dubernet, C. Chauvierre, I. Brigger, and P. Couvreur. Drug delivery to resistant tumors: the potential of poly(alkyl cyanoacrylate) nanoparticles. *J. Control. Rel.* **93**:151–160 (2003).
29. C. Vauthier, C. Dubernet, E. Fattal, H. Pinto-Alphandary, and P. Couvreur. Poly(alkylcyanoacrylates) as biodegradable materials for biomedical applications. *Adv. Drug Deliv. Rev.* **55**:519–548 (2003).
30. C. Cuvier, L. Roblot-Treupel, J. M. Millot, G. Lizard, S. Chevillard, M. Manfait, P. Couvreur, and M. F. Poupon. Doxorubicin-loaded nanospheres bypass tumor cell multidrug resistance. *Biochem. Pharmacol.* **44**:509–517 (1992).
31. S. Bennis, C. Chapey, P. Couvreur, and J. Robert. Enhanced cytotoxicity of doxorubicin encapsulated in polyisohexylcyanoacrylate nanospheres against multidrug-resistant tumour cells in culture. *Eur. J. Cancer* **30A**:89–93 (1994).
32. F. Nemati, C. Dubernet, A. Colin de Verdière, M. F. Poupon, L. Treupel Acar, F. Puisieux, and P. Couvreur. Some parameters influencing cytotoxicity of free doxorubicin loaded nanoparticles in sensitive and multidrug resistant leucemic murine cells: incubation time, number of particles per cell. *Int. J. Pharm.* **102**:55–62 (1994).
33. A. Colin de Verdiere, C. Dubernet, F. Nemati, M. F. Poupon, F. Puisieux, and P. Couvreur. Uptake of doxorubicin from loaded nanoparticles in multidrug-resistant leukemic murine cells. *Cancer Chemother. Pharmacol.* **33**:504–508 (1994).
34. A. Colin de Verdiere, C. Dubernet, F. Nemati, E. Soma, M. Appel, J. Ferte, S. Bernard, F. Puisieux, and P. Couvreur. Reversion of multidrug resistance with polyalkylcyanoacrylate nanoparticles: towards a mechanism of action. *Br. J. Cancer* **76**:198–205 (1997).
35. X. Pepin, L. Attali, C. Domrault, S. Gallet, J. M. Metreau, Y. Reault, P. J. Cardot, M. Imalalen, C. Dubernet, E. Soma, and P. Couvreur. On the use of ion-pair chromatography to elucidate doxorubicin release mechanism from polyalkylcyanoacrylate nanoparticles at the cellular level. *J. Chromatogr. B* **702**:181–191 (1997).
36. R. Mehta and T. G. Burke. Membrane biophysical parameters influencing anthracycline action. In W. Priebe (ed.), *Anthracycline Antibiotics,* ACS Symposium Series 574, American Chemical Society, Washington DC, 1995, pp. 222–240.